Highly active CAR T cells that bind to a juxtamembrane region of mesothelin and are not blocked by shed mesothelin

Xiufen Liu[a,1], Masanori Onda[a,1], Nathan Watson[a], Raffit Hassan[b], Mitchell Ho[a] ⓘ, Tapan K. Bera[a], Junxia Wei[a], Anirban Chakraborty[a], Richard Beers[a], Qi Zhou[a], Asif Shajahan[c], Parastoo Azadi[c], Jingyu Zhan[d] ⓘ, Di Xia[d] ⓘ, and Ira Pastan[a,2] ⓘ

Mesothelin (MSLN) is a cell-surface protein that is highly expressed by many cancers. Despite many clinical trials, there is not a Food and Drug Administration (FDA)-approved antibody-based therapy targeting MSLN. Shed MSLN is present in high concentrations in tumors and in body fluids and constitutes a major barrier to antibody-based therapies. MSLN is shed from cells by the action of proteases that cut very close to the membrane. We have identified the major protease sites in MSLN and prepared a monoclonal antibody (mAb) 15B6, that binds next to the cell membrane at the protease-sensitive region and inhibits MSLN shedding. We determined the structure of a Fab-MSLN peptide complex and found the antibody binds to residues Y-V-DLSMQEL at the C terminus of MSLN. mAb 15B6 makes very active chimeric antigen receptor (CAR) T cells whose activity is not blocked by shed MSLN. The 15B6 CAR T cells have greatly superior antitumor activity in mice than CAR T cells targeting an epitope in shed MSLN.

immunotherapy | cancer | antibody | pancreatic cancer | ovarian cancer

Mesothelin (MSLN) shedding is a barrier to the activity of antibody-based therapeutics targeting MSLN. MSLN is shed from cells by the action of proteases that cut close to the cell membrane. Monoclonal antibody (mAb) 15B6 binds to the protease-sensitive region, inhibits MSLN shedding, and makes very active chimeric antigen receptor (CAR) T cells that are greatly superior in activity in mouse tumor models to CAR T cells made with mAb SS1 that binds to a distal epitope. We ascribe this enhanced activity to binding of 15B6 CAR T cells close to the cell membrane and to avoiding the inhibitory effect of shed MSLN.

MSLN is a lineage-restricted cell-surface protein that is expressed by many cancers and on normal mesothelial cells (1, 2). MSLN was discovered in a search for cell-surface proteins that were expressed in cancers but not on essential organs (3, 4) and is now known to be expressed on many human cancers (1, 2). In addition, patients with high MSLN on their tumors often have a poorer prognosis (1). The specificity and pattern of MSLN expression makes it a popular target for antibody-based therapies, including CAR T cells and bispecific T cell engagers (BiTEs) (5–9). Although a few major responses have been observed with antibody-based therapies targeting MSLN (1, 10, 11), there is not yet a Food and Drug Administration (FDA)-approved drug targeting MSLN.

One major impediment to antibody efficacy is MSLN shedding (12). Shed MSLN inactivates antibodies and antibody-based agents such as CAR T cells and BiTEs before they reach MSLN on the tumor cells. Shedding also releases these agents from the cell surface before they have an opportunity to kill target cells. Previous studies have indicated that MSLN shedding is due to cleavage of MSLN at several different sites close to the cell membrane (12, 13). At least five different enzymes participate in the shedding process and others must exist because for some cell lines no shedding enzymes were identified (13). Another unusual aspect of shedding is that in different cancer cell lines, different enzymes are involved. Up to now ADAM10, ADAM17, BACE1, BACE2, and MMP15 have been identified (13). MSLN levels that result from tumor shedding are much higher inside tumors than in blood (14) and are very high in ascites and pleural fluid of patients with mesothelioma, where the levels can exceed 10 μg/mL. This presents a significant barrier to therapy (15).

Our goal was to acquire quantitative information on the major protease sites resulting in MSLN shedding, to use this information to make a monoclonal antibody that binds to the protease site region, and to use the antibody to make CAR T cells and other targeted therapeutics. We describe here that mAb 15B6, which blocks MSLN shedding, does not react with shed MSLN and makes a very active CAR T cell that produces complete remissions of MSLN-expressing tumors in mice. We ascribe the

Significance

Mesothelin (MSLN) is a cell-surface protein that is a popular target for antibody-based therapies. We have identified shed MSLN as a major obstacle to successful antibody therapies and prepared a monoclonal antibody that inhibits shedding and makes very active CAR T cells whose activity is not blocked by shed MSLN and merits further preclinical development.

¹X.L. and M.O. contributed equally to this work.

²To whom correspondence may be addressed. Email: pastani@mail.nih.gov.
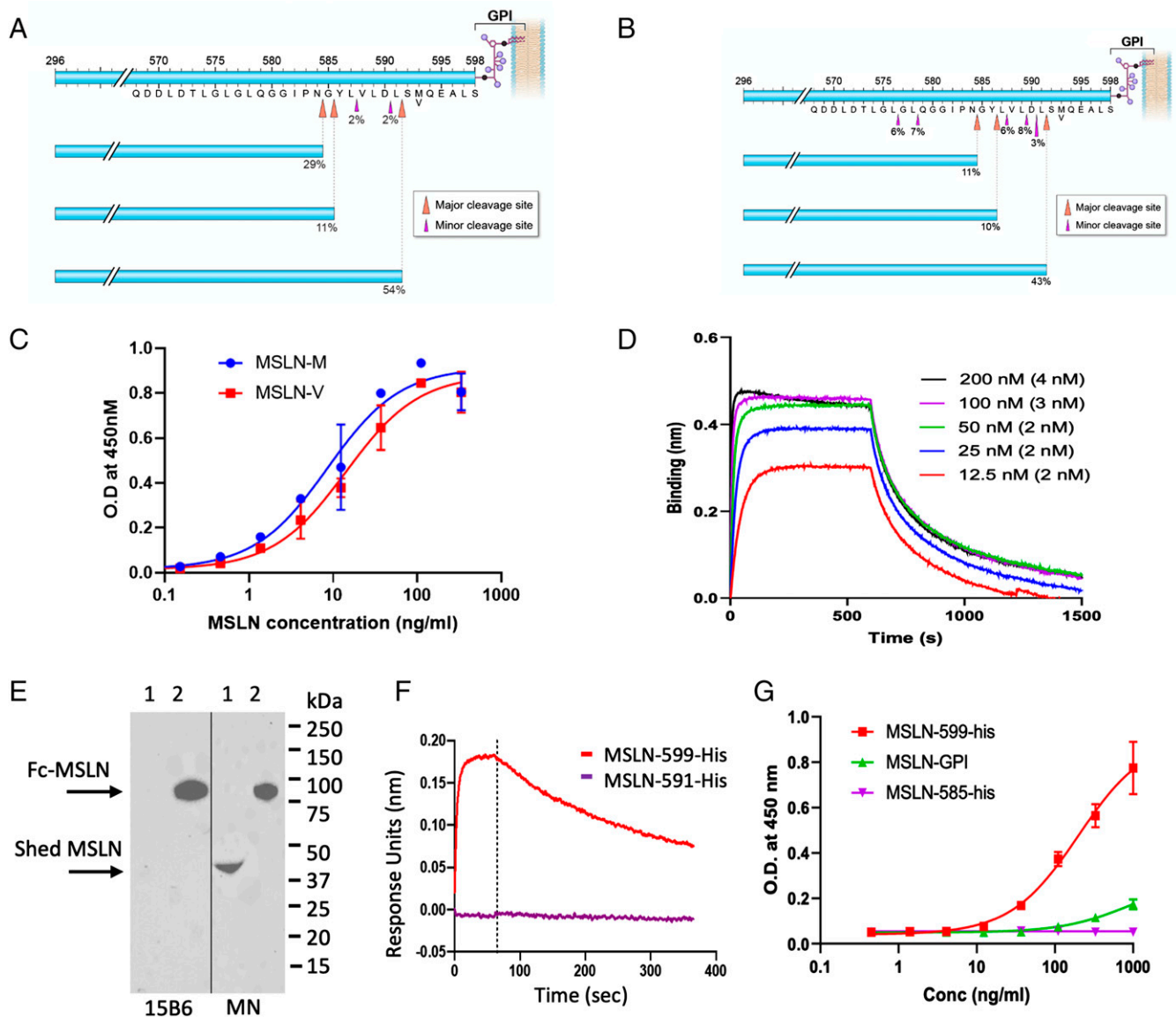
Fig. 1. Major shed species of MSLN and mAb 15B6 binding to various forms of MSLN. (*A* and *B*) Cell culture medium from A431/H9 (*A*) or ascites from a mesothelioma patient (*B*) were purified on an SS1P antibody affinity column and shed MSLN sequence was determined by nano-LC-MS/MS as described in *Materials and Methods*. (*C*) Binding of various concentrations of mAb 15B6 to M and V variants of Fc-MSLN measured by ELISA. (*D*) Binding of Fab of mAb 15B6 to MSLN-His measured by biolayer interferometry (K_D was calculated from individual concentrations). (*E*) Culture medium from OVCAR-8 cells (lane 1) and Fc-MSLN (lane 2) were analyzed by Western blot with either 15B6 or MN. (*F*) Binding of Fab of mAb 15B6 to MSLN–599-his but not to MSLN–585-his measured by biolayer interferometry. (*G*) ELISA measuring binding of mAb 15B6 to MSLN–599-his, MSLN–GPI, and MSLN–585-his.

high activity of the CAR T cells to the fact that mAb 15B6 binds to MSLN at the site where it attaches to the cell membrane and is not inactivated by shed decoy MSLN found at high concentrations inside tumors and in ascites and pleural fluid of cancer patients (14, 15). To the best of our knowledge all other antibodies to MSLN bind to shed MSLN, although the epitopes and the distance from the cell membrane vary among them (16–20).

Results

The MSLN protein is made as a precursor protein of 622 amino acids (*SI Appendix*, Table 1) (21). The 36 amino acid signal sequence is removed and a glycosylphosphatidylinositol (GPI) is attached to position 598, resulting in removal of amino acids 599 to 622 (1). The MSLN protein (37 to 598) is then cleaved by furin after amino acid 295, releasing MPF (37

to 295) from the cell and leaving mature MSLN (296 to 598) attached to the cell membrane by GPI as shown in Fig. 1 *A* and *B*. To obtain the C-terminal sequence of shed MSLN, the protein was affinity purified on a column containing the immunotoxin SS1P (1), which binds strongly to the amino terminus of MSLN, using the ascites of one patient and the medium of A431/H9 cells (15). The purified proteins were subjected to sequence analysis, which revealed the major cut sites (shedding sites) to be after amino acids 584, 586, and 591 in A431/H9 cells (Fig. 1*A*) and at the same sites and minor additional sites (576, 578, and 589) in the ascite samples (Fig. 1*B*). Some of these cut sites were previously identified, but they were not shown to be the major sites of MSLN cleavage (12, 13). Other minor cut sites were also identified (*SI Appendix*, Tables 2 and 3).

To make a mAb reacting with the shedding site region, a peptide from the C terminus of MSLN containing residues
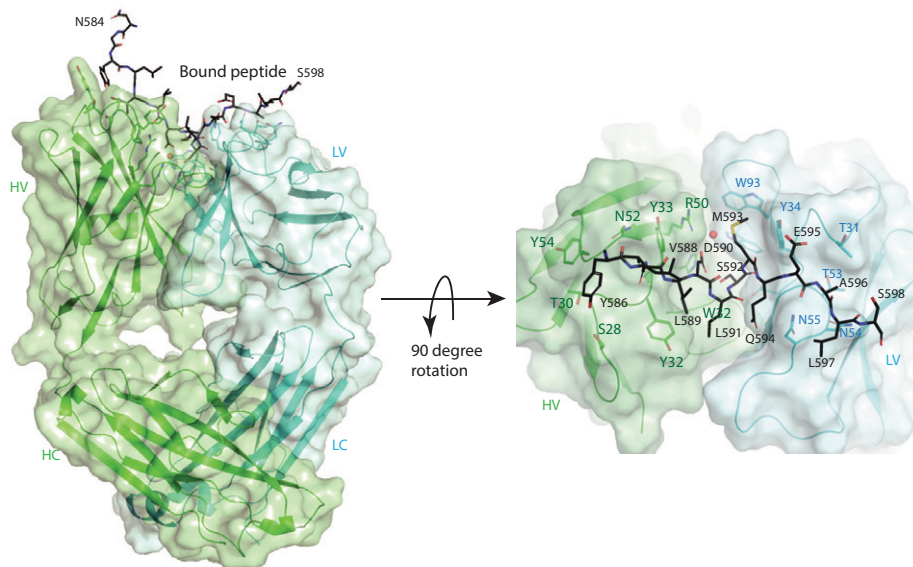
Fig. 2. Crystal structure of the Fab fragment of mAb15B6 in complex with the C-terminal peptide of mesothelin. The heavy (H) and light (L) chains of Fab are rendered as cartoon models and colored in cyan and green, respectively, with the side chains of the critical residues that interact with MSLN peptide shown as stick models and labeled. The constant and variable domains of mAb 15B6 are further indicated as C and V, respectively. Residues from N584 to S598 of the peptide are seen in the crystal structure as rendered on the *Left*. The 90° rotated view is given on the *Right*. The mesothelin peptide from Y586 to L597 forms the binding epitope and is shown as a stick model in black, and the residues are numbered according to their positions in the full-length MSLN sequence. Residues L589, L591, and the terminal S598 have their side chains pointing away from the Fab.

582 to 598 was coupled to keyhole limpet hemocyanin (KLH) and used to immunize mice. This peptide contains all the cut sites. Four hybridomas were isolated that bind to this region. According to the Single Nucleotide Polymorphism Database, the M > V missense variant rs1135210 at position 593 caused by an A-to-G mutation has the allele frequency of 0.3 (22). We found that only one of the mAbs (15B6, IgG2bk) binds to both the M and V variants with high affinity (Fig. 1C) and chose to characterize this mAb, because it is more useful than mAbs reacting only with the M variant. To determine the affinity of the mAb for full-length MSLN, the Fab portion was isolated, and a binding assay using biolayer interferometry was carried out using recombinant MSLN 293 to 599. The data in Fig. 1D show a dissociation constant (K_D) of 2 nM.

To obtain information about the interaction of the MSLN C terminus with mAb 15B6, we crystallized the Fab fragment of the antibody in the presence of a 17-residue MSLN C terminus peptide and determined the structure of the complex at 1.74-Å resolution. The experimental electron density map was fit with a Fab model containing 213 residues for the light (L) and 214 residues for the heavy (H) chains (*SI Appendix,* Fig. 1). There is an extra piece of electron density that spans across the complementarity-determining regions (CDRs) of the Fab, and it was fit with the sequence of the peptide (Fig. 2). The bound peptide is in an extended conformation with the binding epitope, consisting of 12 residues starting from Y586 to L597, among which the side chains of the hydrophobic residues L587 and L589 do not have any contact with the Fab. Careful inspection of the contacts between the peptide and the Fab (*SI Appendix,* Table 4) reveal predominant hydrogen bonding and hydrophilic interactions. The structure permits future rational engineering of antibodies for better interaction with mesothelin.

To determine whether mAb 15B6 reacts with shed MSLN, medium was collected from OVCAR-8 cells and Western blots performed with mAb MN that binds to the amino terminus and mAb 15B6. The data in Fig. 1E show that mAb 15B6 binds strongly to full-length Fc-MSLN (296 to 598) in lane 2 but not to shed MSLN (lane 1). In contrast, mAb MN binds strongly to both shed MSLN and recombinant MSLN (lanes 1 and 2). The sequence of shed MSLN indicates that there are major cleavage sites at 584, 586, and 591. To determine whether mAb 15B6 could bind to this region, we prepared MSLN 296 to 591 and used biolayer interferometry to measure binding affinity. The data in Fig. 1F show no detectable MSLN 296 to 591 binding to the 15B6 Fab, whereas MSLN 296 to 598 binds with high affinity.

To determine whether mAb 15B6 reacts with human cancers, immunohistochemistry studies were performed on several human cancers known to express MSLN. Fig. 3A shows that mAb 15B6 reacts strongly with human mesothelioma, esophageal cancer, lung cancer, and pancreatic ductal cancer tissue samples. Staining of a normal tissue array shows there is no specific cellular reactivity, although there is weak diffuse staining of liver and nonspecific staining of mucous in the stomach (*SI Appendix,* Fig. 2).

Because mAb 15B6 binds to the region where shedding occurs, we examined its ability to inhibit MSLN shedding using eight different cell lines that shed both large and small amounts of MSLN. The data in Fig. 4 A and B show that MSLN shedding is significantly inhibited in all the lines, although the magnitude of shedding inhibition varies from 70 to 80% in OVCAR-8, A431/M18, or CT26M cells to less than 50% in other cell lines. Fig. 4 C–E shows that shedding inhibition is dependent on antibody concentration with 50% inhibition varying from 0.2 to 1 μg/mL in various cell lines.

Cell binding is shown in Fig. 3B and was assessed by flow cytometry using mAb 15B6 or mAb MN. mAb MN was previously shown to strongly bind to cells expressing MSLN (17) . For the cell binding studies, we employed two pancreatic cancers (KLM-1 and T3M4), two mesotheliomas (RH16 and RH29), one ovarian (OVCAR-8), one cervical (HeLa), a colon line transfected with human MSLN (CT26M), and KLM-KO#2, in which the MSLN gene is knocked out (21). As
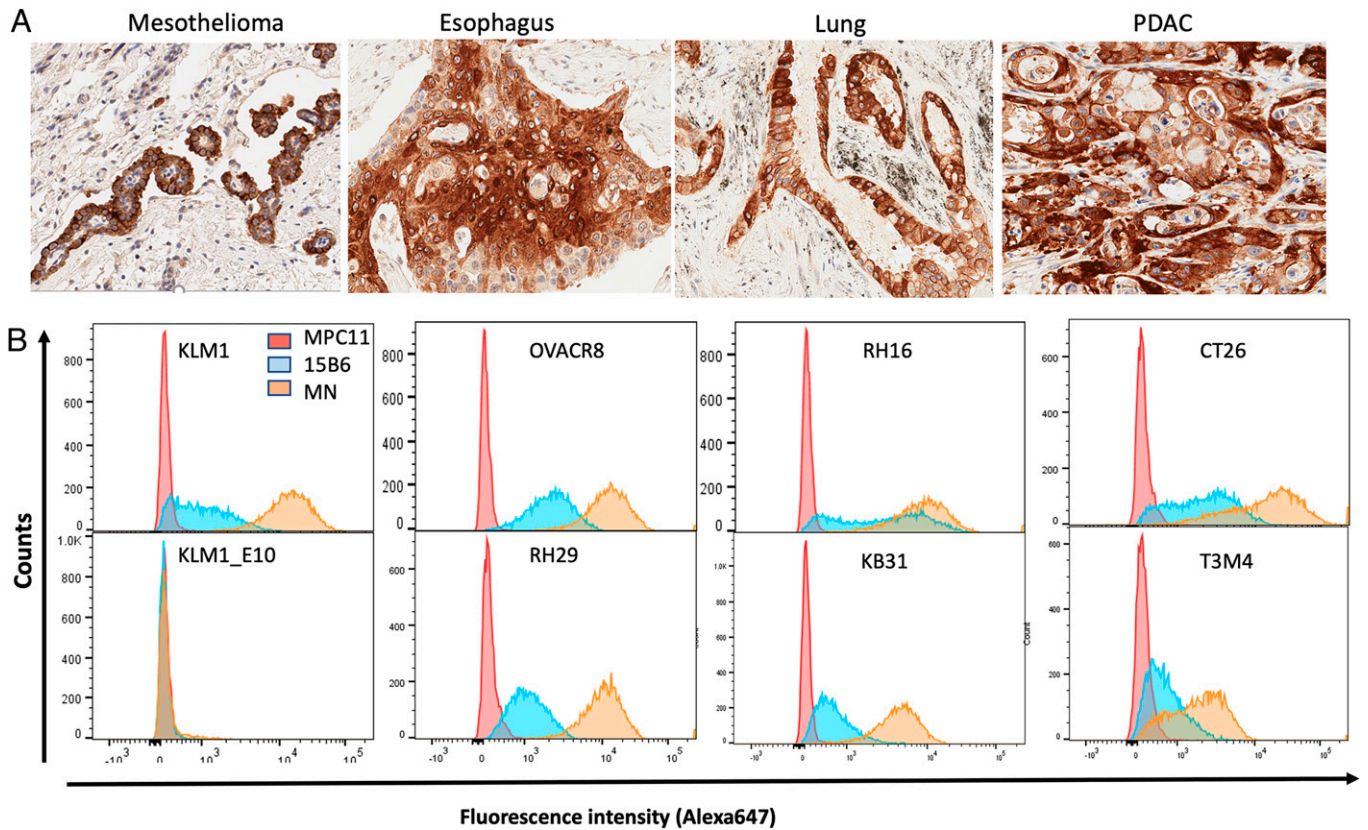
Fig. 3. Binding of mAb 15B6 to fixed tumor samples and to cells. (*A*) Immunohistochemical staining of human tumor samples with mAb 15B6. (*B*) Individual cell lines were analyzed by flow cytometry after staining with either mAb 15B6 or MN as described in *Materials and Methods*.
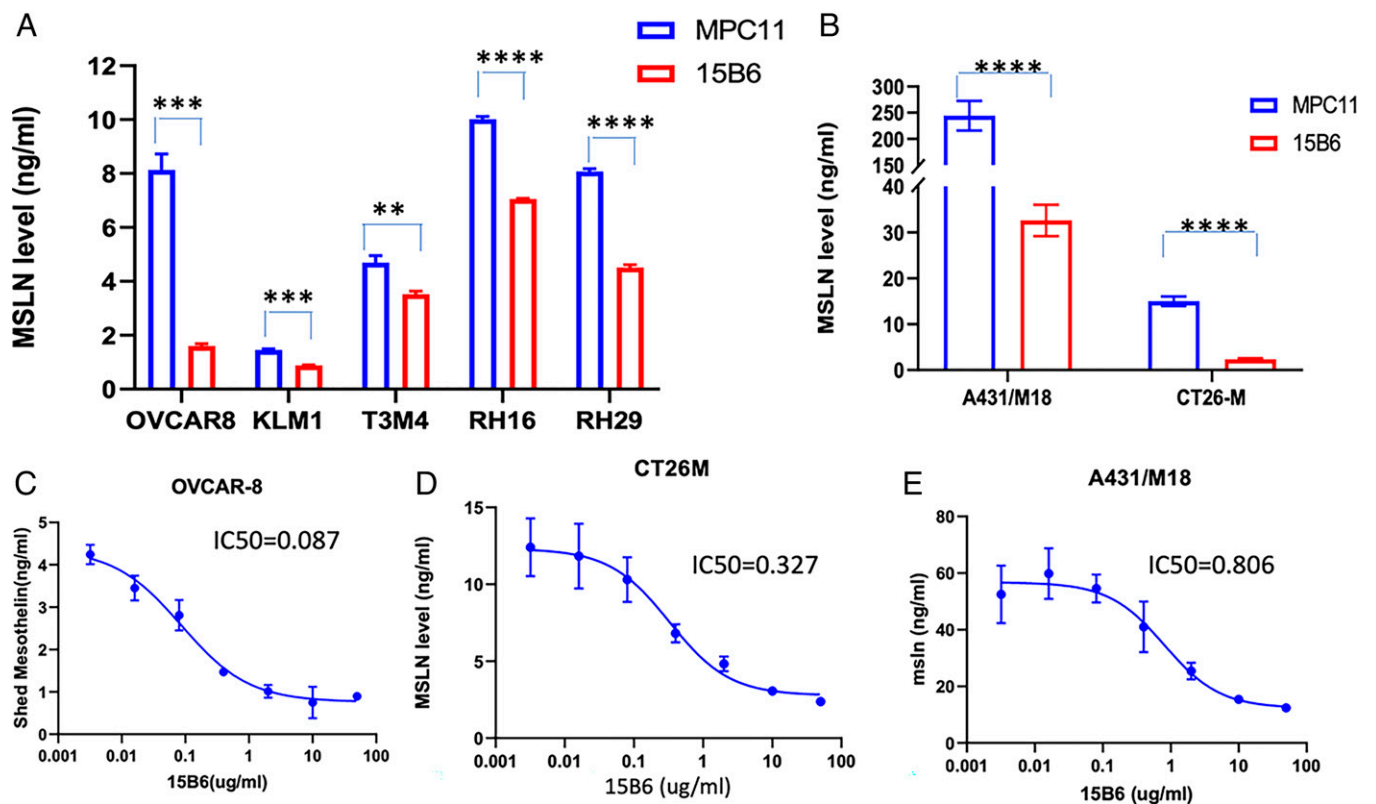
Fig. 4. mAb 15B6 inhibits mesothelin shedding. (*A* and *B*) A total of 50 µg/mL of mAb 15B6 or isotype control MPC 11 was incubated with cells for 24 h. The media were collected and shed MSLN was detected by human mesothelin R-Plex kit. (*C–E*) Different concentrations of mAb 15B6 were incubated with cells for 24 h, medium was collected, and shed MSLN measured by R-Plex kit. *P* values were calculated using multiple *t* tests. *P* value: OVCAR-8 ***P = 0.0004, KLM-1 ***P = 0.0002, T3M4 **P = 0.013, RH16 ****P = 0.00001, RH29 ****P = 0.00001. A431/M18 ****P = 0.0001, CT26-M ****P = 0.00003.
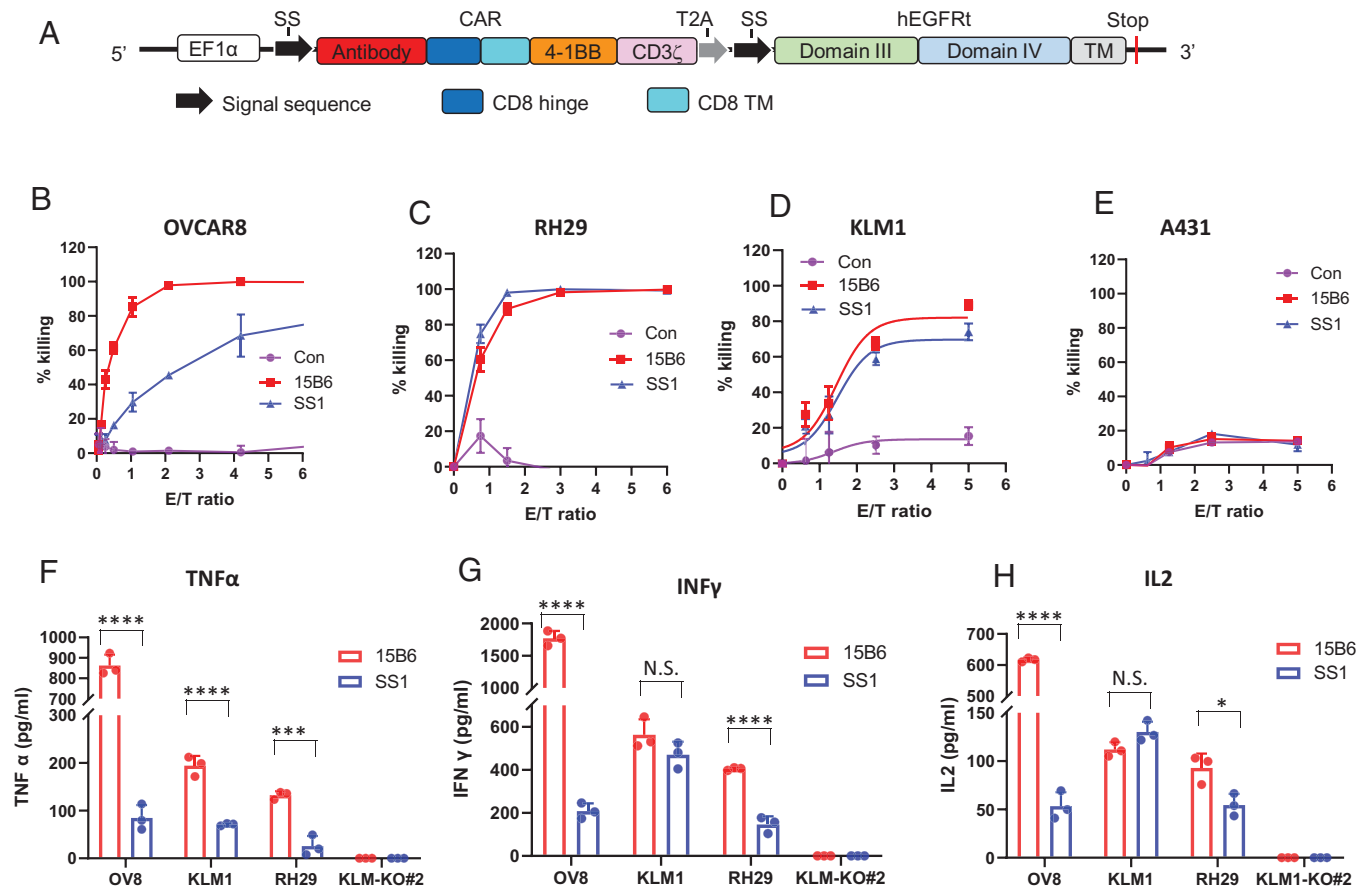
Fig. 5. Killing of MSLN-expressing cancer cells by CAR T cells expressing Fv of 15B6 or SS1. (*A*) Schematic illustration of either 15B6 or SS1 CAR T vector. Antibody is a single chain Fv. In 15B6 CAR T the format is VL-linker-VH-CD8. In SS1 CAR T it is VH-linker-VL-CD8. (*B–E*) Luciferase-expressing OVCAR-8 (*B*), KLM-1 (*C*), RH29 (*D*), or A431 (*E*) cells were cocultured with mock, 15B6, or SS1 CAR-transduced T cells at the indicated E/T ratios for 20 h, and specific lysis was measured using a luminescent-based cytolytic assay. (*F–H*) A total of 5,000 cells were incubated with 15B6 or SS1 CAR T at E/T ratio of 1:1 in 96-well plates. After 24 h, culture media were collected and TNFα (*F*), INFγ (*G*), and IL-2 (*H*) were measured by ELISA (R&D). *P* values were calculated using multiple *t* tests. *P* value: TNFα (*F*) OVCAR-8 *P* = 0.00002, KLM-1 *P* = 0.0005, RH29 *P* = 0.0012; INFγ (*G*) OVCAR-8 *P* = 0.00002, KLM-1 *P* = 0.165, RH29 *P* = 0.0003; IL-2 (*H*) OVCAR-8 *P* < 0.00001, KLM-1 *P* = 0.071, RH29 *P* = 0.024.

expected, mAb MN (orange) binds strongly to all lines except the knockout line. mAb 15B6 (blue) also reacts with all the MSLN-expressing lines, but its reactivity is lower than mAb MN.

Because the epitope to which mAb 15B6 binds is next to the site where GPI is attached to MSLN, we considered the possibility that the GPI at the C terminus interferes with mAb 15B6 binding to cells but not with binding to recombinant MSLN lacking GPI. To investigate this possibility, we prepared MSLN containing GPI by treating A431/H9 cells with phospholipase C and isolating the released protein by affinity chromatography (*SI Appendix*, Fig. 3). The data in Fig. 1*G* are an enzyme-linked immunoassay (ELISA) that shows the binding of mAb 15B6 to MSLN–GPI is much weaker than its binding to MSLN without GPI. In this assay there was no detectable binding to MSLN 296 to 585 lacking the C terminus. This result indicates that decreased binding of mAb 15B6 to cells is due to the presence of GPI, which links MSLN to the cell surface.

CAR T cells that contain the variable fragment (Fv) of mAb 15B6 were produced using the vector developed by the M.H. laboratory (23). In this construct an Fv in which the light chain precedes the heavy chain is fused to a CD8 hinge (Fig. 5*A*). The data in Fig. 5 *B–D* show that 15B6–CAR T cells are very effective in killing OVCAR-8, RH29, and KLM-1 cells. A431 cells, that do not express MSLN, were not specifically killed (Fig. 5*E*). There is also specific killing of other MSLN-positive cells and with different sources of peripheral blood mononuclear cells

(PBMCs) to make the CAR T cells (*SI Appendix*, Fig. 3). When compared with CAR T cells made with the SS1 Fv that binds to the amino terminus of MSLN, the 15B6 cells are much more active in killing OVCAR-8 cells and A431/H9 and slightly but not significantly more active on RH29 and KLM-1 cells (Fig. 5 *B–D* and *SI Appendix*, Fig. 3). There is also enhanced cytokine production in the 15B6 CAR T–treated cultures with the highest levels in OVCAR-8. As expected, there is no increase in cytokines in KLM-1–E10 in which MSLN is knocked out (Fig. 5 *F–H*).

To assess whether shed MSLN can inhibit CAR T function, we added recombinant MSLN with a C-terminal deletion at residue 585 or residue 591, corresponding to the two major shed species (Fig. 1), to OVCAR-8 cells or KLM-1 cells. We then determined whether the cytotoxic activity of CAR T cells containing 15B6 Fv or SS1 Fv is blocked. The data in Fig. 6*A* show that the 585 MSLN deletion blocks the activity of SS1 CAR T cells on OVCAR-8 cells but not the activity of 15B6 CAR T cells. The data in Fig. 6*B* show that the 591 MSLN deletion also blocks the activity of SS1 CAR T cells on OVCAR-8 cells but not the activity of 15B6 CAR T cells. The data in Fig. 6 *C* and *D* show similar experiments. Fig. 6*C* shows that the 585 MSLN deletion blocks the activity of SS1 CAR T cells on KLM-1 cells, but not the activity of 15B6 CAR T cells, and the data in Fig. 6*D* show that the 591-deletion protein also blocks the activity of SS1 CAR T cells on KLM-1
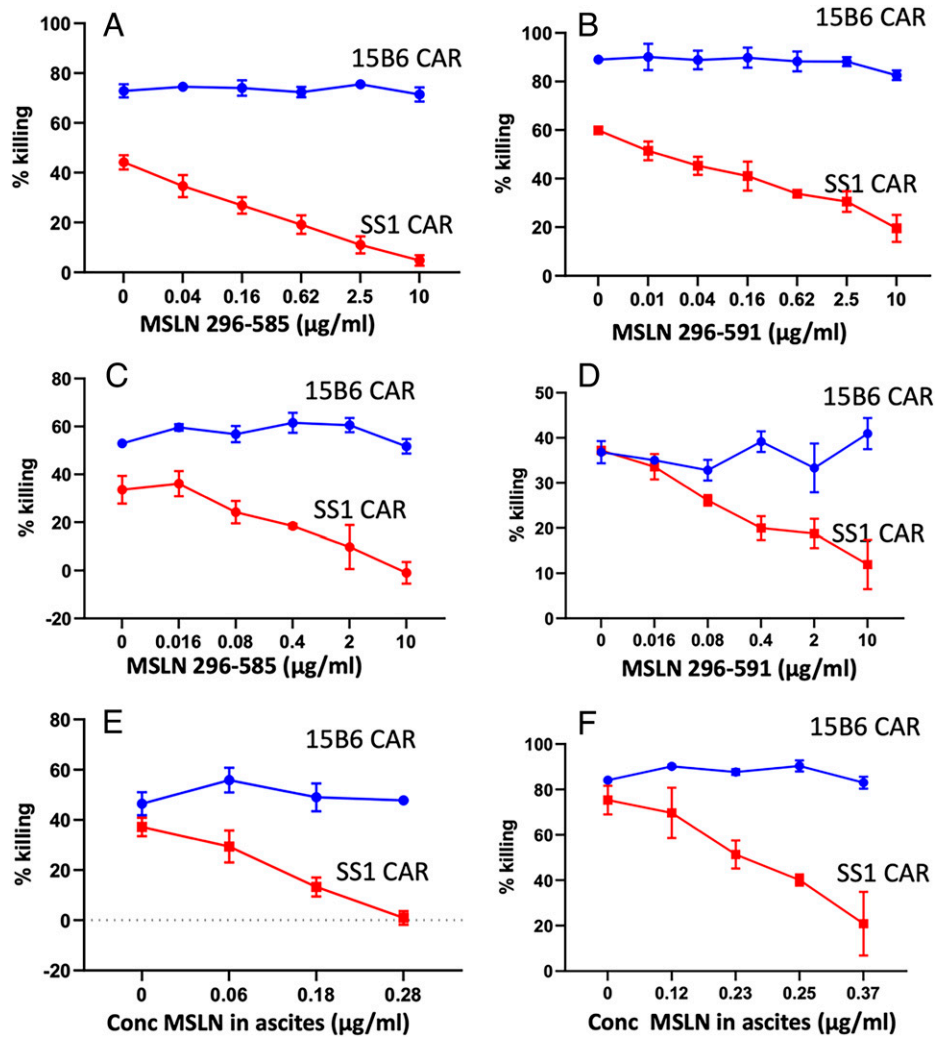
Fig. 6. Truncated mesothelin (295 to 595 or 295 to 591) and an ascites sample block activity of SS1 CAR T but not 15B6 CAR T. (*A* and *B*) OVCAR-8 cells were incubated with 15B6 or SS1 CAR T cells: (*A*) MSLN (295 to 585) and (*B*) MSLN (295 to 591). (*C* and *D*) KLM-1 cells were incubated with 15B6 or SS1 CAR T cells: (*C*) MSLN (295 to 585) and (*D*) MSLN (295 to 591). (*E*) KLM-1 cells were incubated with 15B6 or SS1 CAR T cells and ascites containing various amounts of MSLN. (*F*) RH29 cells were incubated with 15B6 or SS1 CAR T cells and ascites containing various amounts of MSLN. After 24 h, cell killing was measured by a luminescent-based cytolytic assay. The concentration on the horizontal axis shows the final concentration of MSLN present in each well.

cells but not the activity of 15B6 CAR T cells. In both cancer cell lines, the inhibition of SS1 CAR T cells is dose dependent.

Ascites from patients with mesothelioma have high levels of MSLN (15). We evaluated the ability of an ascites sample to inhibit CAR T cell activity on KLM-1 cells and mesothelioma RH29 cells. The data in Fig. 6 *E* and *F* show that the ascites inhibits killing by the SS1 CAR T cells in a concentration-dependent manner but not 15B6 CAR T cells. Inhibition by 50% was in the range of 0.3 to 0.5 µg/mL for SS1 CAR T cells, corresponding to the levels of inhibition by recombinant MSLN (Fig. 6 *A–D*).

Having shown that the 15B6 CAR T cells are very cytotoxic to cell lines, we performed several experiments in mice with MSLN-expressing tumors. Representative experiments are shown in Fig. 7. Fig. 7 *A* and *B* shows an experiment with KLM-1 tumors. The 15B6 CAR T cells were given on day 14 when the tumors are well established and growing. We found that 15B6 CAR T cells caused the tumor signal to rapidly disappear and to remain absent until day 40 when the mice were killed. There was a very small response with the SS1 CAR T cells in this model. Fig. 7 *C* and *D* shows that 15B6 CAR T cells given on day 14 also caused complete regressions of

OVCAR-8 tumors that lasted until day 56 when the mice were killed. There was no significant response with tumors treated with SS1 CAR T cells and the mice had to be killed early because of cancer progression.

Discussion

A major factor contributing to the failure of antibody-based therapies targeting MSLN-expressing tumors is the presence of large amounts of shed MSLN in body fluids that can prevent these agents from reaching tumor cells (12, 15). In addition, shedding releases antibody-based therapeutics from target cells before they have a chance to act (24). In the ascites and pleural fluid of mesothelioma patients, MSLN levels are very high, ranging up to 15 µg/mL (15). To overcome the shed MSLN barrier, we isolated mAb 15B6 that binds to a juxtamembrane region of MSLN and does not bind to shed MSLN. Structural studies show that mAb 15B6 interacts with residues Y-V-DLSMQEL at the C terminus of MSLN. Many anti-MSLN antibodies have been previously described and used to make CAR T cells. The initial antibodies against MSLN, K1 and SS1 (used to make MORAb-009), react with the disordered amino
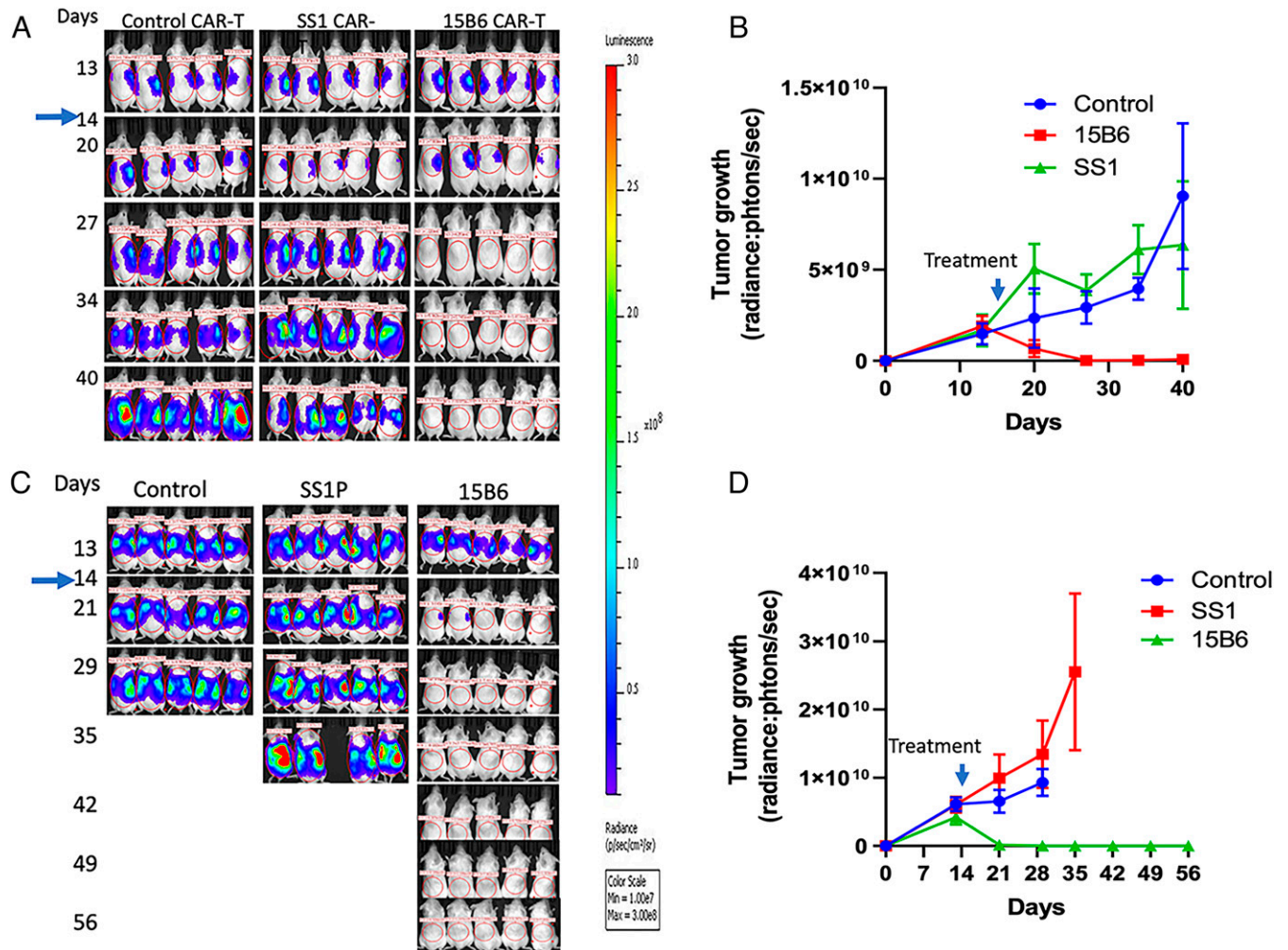
Fig. 7. The 15B6 CAR T cells are more active than SS1 CAR T cells in mice. Five million KLM1-luc cells (*A* and *B*) or OVCAR8-luc cells (*C* and *D*) were injected into mice intraperitoneally. On day 14, 5 million mock, 15B6, or SS1 CAR T cells were injected intravenously. Dorsal images of mice were measured every week by bioluminescent imaging (*n* = 5 per group). (*B* and *D*) Quantitation of bioluminescence in mice treated in *A* and *C*. Values represent mean ± SEM.

terminal domain (3, 16), To isolate antibodies to other regions of MSLN, we immunized rabbits with human MSLN and identified 231 hybridomas that bind to MSLN. Remarkably 223/231 recognize the amino end, five mAbs bind to the central region, and only three to the membrane-proximal region (19). One mAb that reacts with the membrane proximal region (YP218) was humanized and used to make CAR T cells (25). These CAR T cells are very active, probably because the epitope is closer to the cell membrane than that of SS1 Fv. The first CAR T cells against MSLN used the SS1 Fv that binds to the amino end of MSLN (26). This mAb binds in the same region where MUC16 binds (27), and SS1 binding can be displaced by MUC16 in vitro (27). In patients receiving MORAb-009 that contains the SS1 Fv, MUC16 levels rise showing that there is also competition in vivo (28). CAR T cells targeting other regions of MSLN have been developed but the epitopes targeted are all present in shed MSLN. mAb M5 binds to amino acids 485 to 507, 532 to 537, and 545 to 572 (18); mAb YP218 binds to 525 to 560 (19); and mAb#3 binds to 546 to 573 (20). Asgarov et al. used MSLN Pro291-Asp590 as their immunogen (29). It is unlikely their antibody binds to the same epitope as mAb 15B6, since mAb 15B6 does not bind to MSLN 295 to 591 (Fig. 1*F*).

To assess whether CAR T cells containing mAb 15B6 were superior in activity to a CAR T targeting epitopes in shed

MSLN, we did a head-to-head comparison of 15B6 CAR T cells with cells containing the SS1 Fv, which binds to the amino terminus of MSLN and was the first anti-MSLN antibody used for CAR T production (26). We found in cell culture that 15B6 CAR T cells are about twofold more active than SS1 CAR T cells in killing OVCAR-8 cells that shed large amounts of MSLN, and are only slightly more active on cells that shed less MSLN (Fig. 5). However, in mice, the difference between the two types of CAR T cells was very large. 15B6 CAR T cells produced complete remissions of OVCAR-8 and KLM1 tumors, whereas SS1 CAR T cells are much less active or inactive, only producing transient slowing of tumor growth (Fig. 7).

We attribute the difference between 15B6 and SS1 CAR T activity to several factors (Fig. 8). We believe the most important factor is the accumulation of free MSLN inside tumors that prevents access to cells; shed MSLN can interfere with SS1 Fv binding to cells but cannot interfere with 15B6 binding. The second is that mAb 15B6 binds at a juxtamembrane portion of MSLN where it attaches to GPI. Proximity to the membrane is very important for CAR T cell killing (30–33). Finally, MSLN is constantly shed by cells and shedding will release antibodies that are bound to most regions of MSLN.

Although this paper focuses on the use of mAb 15B6 for CAR T cells, it is also being used to develop other types of
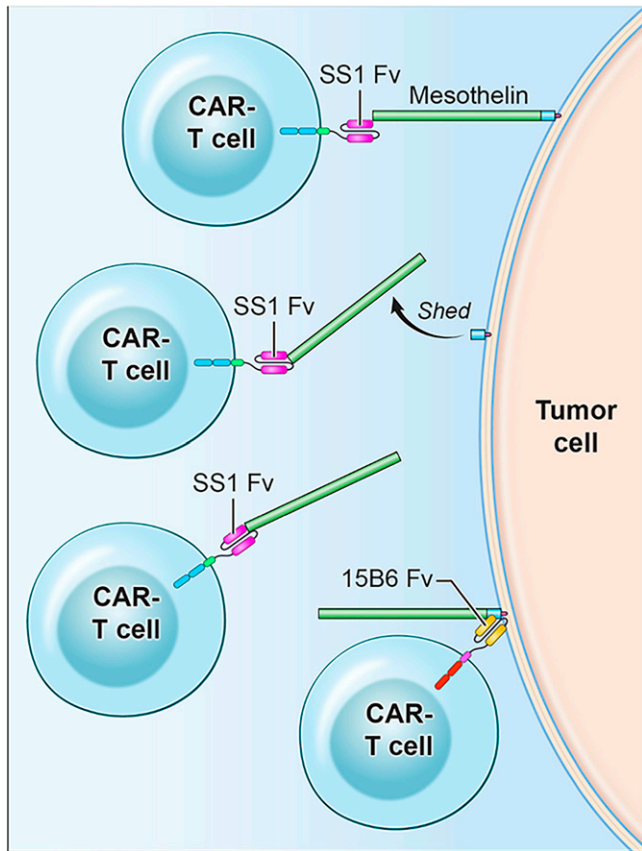
Fig. 8. Cartoon comparing mechanism of action of SS1 CAR T cells with 15B6 CAR T cells. SS1 CAR T cell binds to MSLN at a site distant from the cell membrane, is released by MSLN shedding, and binds to shed MSLN. 15B6 CAR T cell binds to cell-associated MSLN at the plasma membrane and is not released.

engineered cells as well as bispecific antibodies (BiTEs) targeting MSLN and CD3 (7). Blinatumomab, which targets CD19, has received FDA approval for treatment of acute lymphoblastic leukemia (ALL) (34). Blinatumomab can only be given at low doses to patients because high doses produce cytokine storms as a serious side effect. We expect that shed MSLN, which can occur in body fluids at concentrations as high as 1 to 10 μg/mL, will be a serious barrier to MSLN-targeting BiTEs, if like Blinatumomab, they can only be given at a total dose of about 28 μg per day.

In summary, mAb 15B6 binds to a juxtamembrane region of MSLN, inhibits MSLN shedding, and makes very active CAR T cells whose activity is not blocked by truncated or shed MSLN. 15B6 CAR T cells produce complete remissions in several tumor models and are greatly superior in antitumor activity to CAR T cells that bind to the amino terminus of MSLN. The CAR T Fv of mAb 15B6 has been humanized and the cells are ready for further clinical development.

Materials and Methods

Cell Culture. OVCAR-8, KB31, KLM-1, T3M4, A431/H9, RH16, RH29, CT26M, and KLM-1 KO#2 cells were described before (12, 13, 21). For A431/M18, A431 human epidermoid carcinoma cells were transfected with pcDNA3.1(+) vector containing a full-length mesothelin (593M) cDNA by Lipofectamine (Invitrogen). We selected a high-expression clone stably expressing mesothelin (A431/M18) with a limiting dilution method. The luciferase (luc)-expressing cell lines OVCAR8-luc, KLM1-luc, A431-luc, RH29-luc, and KLM-1 KO#2-luc were acquired from R.H., M.H., and C. Alewine, NCI (Bethesda, MD). All cells were cultured in RPMI-1640 medium. Culture media were supplemented with 10% fetal bovine serum (FBS) and 1% penicillin–streptomycin. Cells were maintained at 5% CO_2 at 37 °C.

Purification and Quantification of Shed MSLN. To isolate shed MSLN, an anti-MSLN column was prepared by covalently immobilizing 2 mg of SS1P, an anti-MSLN recombinant immunotoxin (1) on a 1-mL column packed with N-hydroxy-succinimide activated Sepharose resin. Shed MSLN derived from either A431/H9 cell culture supernatant or human ascites were then passed over the prepared anti-MSLN column. After washing the column with 10 column volumes of phosphate buffered saline (PBS), nonspecific binding proteins were removed by washing with sodium acetate buffer, pH 5.0, and MSLN was eluted with acetate buffer pH 3.0 followed by immediate neutralization in 1 M Tris·HCl pH 8.0 buffer. Purified MSLN was analyzed using nanoliquid chromatography tandem mass spectrometry (nano-LC-MS/MS). Briefly, affinity-purified samples were reduced, alkylated, digested with trypsin, and analyzed via nano-LC-MS/MS. To quantify the C-terminal composition, the area under the curve of each peak was calculated to measure the relative percent composition of each C-terminal peptide.

Establish Hybridoma 15B6 against the C-Terminal Region of MSLN. To make mAbs reacting with the C terminus of MSLN, we immunized mice with C-582-IPNGYLVLDLSMQEALS-598 in which the cysteine was used to couple the peptide to KLH. Ten Balb/c mice were immunized and after five immunizations, the mouse sera were screened by ELISA to determine their reactivity with the peptide; two mice with high titers were used to prepare hybridomas. Spleen cells were fused with mice myeloma cells, SP2/O. Fifteen hybridomas were expanded and those reacting with MSLN(M)-Fc and/or MSLN(V)-Fc were expanded and subcloned. Among these 15 hybridomas, 15B6 showed the best binding to both MSLN(M)-Fc and MSLN(V)-Fc on ELISA and to cells expressing MSLN by flow cytometry. The sequence of mouse 15B6 were shown in *SI Appendix*, Table 5.

mAb 15B6 Binding to MSLN Fc Protein by ELISA. ELISA plates were coated with MSLN(M)-Fc or MSLN(V)-Fc (1 μg/mL, 50 μg/well). After washing, mAb 15B6 was added at various concentrations, and bound antibody was detected with horseradish peroxidase conjugated goat anti-mouse IgG (H+L); 115-035-146; Jackson ImmunoResearch), followed by 3,3',5,5'-Tetramethylbenzidine substrate (Thermo Fisher) and stopped with 2 M sulfuric acid. Optical density was measured with a plate reader.

Biolayer Interferometry Binding Assays. Assays were performed as previously described (23). The binding kinetics were performed using the Octet RED96 system (FortéBio) at the Biophysics core at National Heart, Lung, and Blood Institute. Various his-tagged MSLN proteins were immobilized onto Ni-NTA biosensors (FortéBio) and their binding to 15B6 Fab was measured with biolayer interferometry. Binding data were analyzed with GraphPad Prism.

Isolation of GPI-Linked MSLN and Detection of MSLN–GPI Binding to 15B6. GPI–MSLN was produced by incubating A431/H9 cells in phosphatidylinositol-specific phospholipase C (PI-PLC) (0.5 unit/mL) in serum-free media for 3 h at room temperature. Cell culture supernatant containing GPI–MSLN released by PI-PLC were then filtered, purified, washed, and eluted with anti-MSLN chromatography as described above. The size of GPI–MSLN was compared with shed MSLN on a nonreducing sodium dodecyl sulfate–polyacrylamide gel electrophoresis (SDS-PAGE) gel (*SI Appendix*, Fig. 4). An ELISA was performed to measure the binding of MSLN–GPI to mAb 15B6. A total of 50 μL of 1 μg/mL of MSLN–599-his, MSLN–585-his, or MSLN–GPI were coated on wells of a 96-well dish overnight. After blocking and washing, mAb 15B6 was added at indicated concentrations overnight, and bound antibody was detected as described in the ELISA method.

Shedding Inhibition Assay. A total of 15,000 cells per well were seeded in 96-well plates. After 24 h, cells were washed and mAb 15B6 or MPC-11 was added at indicated concentrations and incubated with cells; 24 h later, culture media were collected and cleared by centrifugation. Shed MSLN was measured by a human MSLN R-Plex kit (Mesoscale Discovery).

Generation and Expansion of CAR T Cells. Plasmid DNA expressing second generation CAR T cells was packaged into lentivirus (Genetic Core, NIH) and transduced into human PBMCs stimulated with anti-CD3/CD28-Dynabeads (Thermo Fisher) and 300 U/mL of IL-2 in RPMI medium. The transduced PBMCs were fed with fresh medium containing IL-2 (Miltenyi Biotec) every other day. On day 8 or 9, they were analyzed for transduction efficiency by staining anti-EGFR-PE (R&D) and anti-CD3 using flow cytometry. The cells were collected for cytotoxicity assays or frozen before day 11 (23).

Luminescent-Based Cytolytic Assay. Effector CAR T cells were cocultured with luciferase-expressing target cells at different effector/target (E/T) ratios for 20 h. At the end of the coculture period, supernatant was saved for cytokine assays of IFN-γ, TNF-α, or IL2 levels (R&D Systems). The remaining tumor cells were lysed for 10 min. The luciferase activity in the lysates was measured using the Steady Glo luciferase assay system on Victor (PerkinElmer). Results were analyzed as percent killing based on luciferase activity in wells with tumor cells alone: % killing = 100 − (relative light units [RLU] from wells with effector and target cells)/(average RLU from wells with target cells) × 100.

Western Blotting. Cell pellets were prepared in lysis buffer containing 50 mM Tris HCl, 150 mM NaCl, 5 mM ethylenediamine tetra acetic acid with 1% Nonidet P-40, and protease inhibitors. SDS-PAGE was run with equal amounts of protein, on a NuPAGE 4 to 12% Bis-Tris gel under reducing conditions. Protein was transferred onto a nitrocellulose membrane and subjected to Western blot analysis using appropriate antibodies (13).

Detection of Surface MSLN Expression by Flow Cytometry. Cells were harvested and stained with either 15B6 or MN antibody conjugated to Alexa Fluor-647 and analyzed using a FACSCanto II flow cytometer. A total of 10,000 counts were collected and analyzed using the FlowJo v10.4.2 software.

Animal Studies. A total of 5 million OVCAR-8 or KLM-1 luciferase-expressing cells were implanted intraperitoneally (I.P.) into 6- to 10-wk-old NOD SCID gamma mice. On day 7 or 14, mice were injected with a single dose of 5×10^6 mock transfected T cells, SS1 CAR T cells, or 15B6 CAR T cells by tail vein. Tumors were imaged using Xenogen IVIS Lumina (PerkinElmer) after I.P. injection of 1.5 mg d-luciferin (PerkinElmer). Living Image software was used to analyze the bioluminescence signal flux for each mouse as radiance:photons per second. Mice were killed when they showed any sign of sickness. All mice were housed and treated under the protocol approved by the Institutional Animal Care and Use Committee at the NIH.

Data Availability. The mass spectrometry proteomics data have been deposited to the ProteomeXchange Consortium via the PRIDE partner repository with the dataset identifier PXD033137 (35). All other study data are included in the article and/or *SI Appendix*.

1. R. Hassan *et al.*, Mesothelin immunotherapy for cancer: Ready for prime time? *J. Clin. Oncol.* **34**, 4171–4179 (2016).
2. N. G. Ordóñez, Application of mesothelin immunostaining in tumor diagnosis. *Am. J. Surg. Pathol.* **27**, 1418–1428 (2003).
3. K. Chang, I. Pastan, M. C. Willingham, Isolation and characterization of a monoclonal antibody, K1, reactive with ovarian cancers and normal mesothelium. *Int. J. Cancer* **50**, 373–381 (1992).
4. K. Chang, I. Pastan, Molecular cloning of mesothelin, a differentiation antigen present on mesothelium, mesotheliomas, and ovarian cancers. *Proc. Natl. Acad. Sci. U.S.A.* **93**, 136–140 (1996).
5. A. Morello, M. Sadelain, P. S. Adusumilli, Mesothelin-targeted CARs: Driving T cells to solid tumors. *Cancer Discov.* **6**, 133–146 (2016).
6. A. Klampatsa, V. Dimou, S. M. Albelda, Mesothelin-targeted CAR-T cell therapy for solid tumors. *Expert Opin. Biol. Ther.* **21**, 473–486 (2021).
7. M. E. Molloy *et al.*, Preclinical characterization of HPN536, a trispecific, T-cell-activating protein construct for the treatment of mesothelin-expressing solid tumors. *Clin. Cancer Res.* **27**, 1452–1462 (2021).
8. G. L. Beatty *et al.*, Activity of mesothelin-specific chimeric antigen receptor T cells against pancreatic carcinoma metastases in a phase 1 trial. *Gastroenterology* **155**, 29–32 (2018).
9. P. S. Adusumilli *et al.*, A phase I trial of regional mesothelin-targeted CAR T-cell therapy in patients with malignant pleural disease, in combination with the anti-PD-1 agent pembrolizumab. *Cancer Discov.* **11**, 2748–2763 (2021).
10. R. Hassan *et al.*, Major cancer regressions in mesothelioma after treatment with an anti-mesothelin immunotoxin and immune suppression. *Sci. Transl. Med.* **5**, 208ra147 (2013).
11. D. Yeo, I. Castelletti, N. van Zandwijk, J. E. J. Rasko, Hitting the Bull's-eye: Mesothelin's role as a biomarker and therapeutic target for malignant pleural mesothelioma. *Cancers (Basel)* **13**, 3932 (2021).
12. Y. Zhang, O. Chertov, J. Zhang, R. Hassan, I. Pastan, Cytotoxic activity of immunotoxin SS1P is modulated by TACE-dependent mesothelin shedding. *Cancer Res.* **71**, 5915–5922 (2011).
13. X. Liu, A. Chan, C. H. Tai, T. Andresson, I. Pastan, Multiple proteases are involved in mesothelin shedding by cancer cells. *Commun. Biol.* **3**, 728 (2020).
14. Y. Zhang, L. Xiang, R. Hassan, I. Pastan, Immunotoxin and taxol synergy results from a decrease in shed mesothelin levels in the extracellular space of tumors. *Proc. Natl. Acad. Sci. U.S.A.* **104**, 17099–17104 (2007).
15. J. Zhang *et al.*, Loss of mesothelin expression by mesothelioma cells grown in vitro determines sensitivity to anti-mesothelin immunotoxin SS1P. *Anticancer Res.* **32**, 5151–5158 (2012).
16. J. Ma, W. K. Tang, L. Esser, I. Pastan, D. Xia, Recognition of mesothelin by the therapeutic antibody MORAb-009: Structural and mechanistic insights. *J. Biol. Chem.* **287**, 33123–33131 (2012).
17. M. Onda *et al.*, New monoclonal antibodies to mesothelin useful for immunohistochemistry, fluorescence-activated cell sorting, Western blotting, and ELISA. *Clin. Cancer Res.* **11**, 5840–5846 (2005).
18. G. Beatty *et al.*, "Human Mesothelin Chimeric Antigen Receptors and Uses Thereof." US Patent WO2015090230A1 (2015).
19. Y. F. Zhang *et al.*, New high affinity monoclonal antibodies recognize non-overlapping epitopes on mesothelin for monitoring and treating mesothelioma. *Sci. Rep.* **5**, 9928 (2015).
20. E. Hatterer *et al.*, Targeting a membrane-proximal epitope on mesothelin increases the tumoricidal activity of a bispecific antibody blocking CD47 on mesothelin-positive tumors. *MAbs* **12**, 1739408 (2020).
21. L. R. Avula *et al.*, Mesothelin enhances tumor vascularity in newly forming pancreatic peritoneal metastases. *Mol. Cancer Res.* **18**, 229–239 (2020).
22. S. T. Sherry, M. Ward, K. Sirotkin, dbSNP-database for single nucleotide polymorphisms and other classes of minor genetic variation. *Genome Res.* **9**, 677–679 (1999).
23. N. Li *et al.*, CAR T cells targeting tumor-associated exons of glypican 2 regress neuroblastoma in mice. *Cell Rep Med* **2**, 100297 (2021).
24. P. Awuah, T. K. Bera, M. Folivi, O. Chertov, I. Pastan, Reduced shedding of surface mesothelin improves efficacy of mesothelin-targeting recombinant immunotoxins. *Mol. Cancer Ther.* **15**, 1648–1655 (2016).
25. Z. Zhang *et al.*, Modified CAR T cells targeting membrane-proximal epitope of mesothelin enhances the antitumor function against large solid tumor. *Cell Death Dis.* **10**, 476 (2019).
26. C. Carpenito *et al.*, Control of large, established tumor xenografts with genetically retargeted human T cells containing CD28 and CD137 domains. *Proc. Natl. Acad. Sci. U.S.A.* **106**, 3360–3365 (2009).
27. O. Kaneko *et al.*, A binding domain on mesothelin for CA125/MUC16. *J. Biol. Chem.* **284**, 3739–3749 (2009).
28. R. Hassan *et al.*, Phase I clinical trial of the chimeric anti-mesothelin monoclonal antibody MORAb-009 in patients with mesothelin-expressing cancers. *Clin. Cancer Res.* **16**, 6132–6138 (2010).
29. K. Asgarov *et al.*, A new anti-mesothelin antibody targets selectively the membrane-associated form. *MAbs* **9**, 567–579 (2017).
30. K. L. S. Cleary, H. T. C. Chan, S. James, M. J. Glennie, M. S. Cragg, Antibody distance from the cell membrane regulates antibody effector mechanisms. *J. Immunol.* **198**, 3999–4011 (2017).
31. W. Haso *et al.*, Anti-CD22-chimeric antigen receptors targeting B-cell precursor acute lymphoblastic leukemia. *Blood* **121**, 1165–1174 (2013).
32. J. Li *et al.*, Membrane-proximal epitope facilitates efficient T cell synapse formation by anti-FcRH5/CD3 and is a requirement for myeloma cell killing. *Cancer Cell* **31**, 383–395 (2017).
33. W. Xiong *et al.*, Immunological synapse predicts effectiveness of chimeric antigen receptor cells. *Mol. Ther.* **26**, 963–975 (2018).
34. Center for Drug Evaluation and Research, U.S. Food and Drug Administration, Blincyto BLA 125557 approval letter. Center for Drug Evaluation and Research (2014).
35. Y. Perez-Riverol *et al.*, The PRIDE database resources in 2022: a hub for mass spectrometry-based proteomics evidences. *Nucleic Acids Res.* **50**, D543–D552 (2022).